Published in IET Science, Measurement and Technology
Received on 26th May 2008
Revised on 6th January 2009
doi: 10.1049/iet-smt:20080122

ISSN 1751-8822

Numerical investigation on compact multimode dielectric resonator antennas of very high permittivity

M. Rotaru J.K. Sykulski

School of ECS, University of Southampton, Highfield, Southampton, SO17 1BJ, UK
E-mail: jks@soton.ac.uk

Abstract: An electrically small antenna based on a dielectric resonator antenna (DRA) is investigated. Two well-known simulation techniques, the finite element method and the finite integration technique have been applied to study a low volume high permittivity DRA. It is demonstrated that the design of a compact size and wide frequency coverage DRA for 2.4–2.5 GHz ISM frequency band is possible by proper selection of the resonator shape in combination with appropriate resonant modes. Numerical results for one particular antenna design are reported.

1 Introduction

In the last decade, the need for small size and wide band antennas has increased tremendously, driven especially by the huge demand of mobile and portable communication systems. Antennas and RF front-end stage are key components that often control the overall performance of the wireless systems. Cost, size and weight are the most important factors that can determine the success or failure of wireless technology, unlike, say, in military applications where performance is the main consideration. These factors are even more critical when several wireless technologies – such as GPS, GSM, UWB, Bluetooth and/or WLAN – are integrated in a multi-functional device. Each of these technologies has its own frequency band (Table 1) and might need its unique antenna and its own RF front end. It is imperative that small antennas have both a wide band and a multi-frequency response.

An electrically small antenna, as described first by Wheeler in 1940 [2] can be defined as an antenna that can fit inside a hypothetical sphere with a radius $a = 1/k$ where k is the wave number. In fact the antennas used for portable wireless devices may often be considered to be electrically small. One of the characteristics of electrically small antennas is that they have far-field characteristics similar to an electric or a magnetic dipole, or a combination of both. Although the far-field radiation pattern is comparable with the dipole (electric or magnetic) the near field of a small antenna is significantly different from that of a simple dipole. It is also essential to appreciate that the near field distribution of a small antenna affects its performance. One of the effects of the size reduction of the antenna is a drop in the radiated power (P_{rad}); in fact the radiated power decreases faster than the energy stored and power loss in the antenna structure. Also, because of the size reduction, which is below its resonant size, the structure will store energy in the near field that can be electric or magnetic, depending on the antenna type. Therefore for this type of an antenna, it is essential to have a reactive lumped element (capacitor or inductor) in its feed, to cancel the reactive input impedance at the frequency of interest. This will change the total input impedance of the antenna that now has a form of a resonator. For such a resonator a quality factor Q can be defined

$$Q = \frac{\omega W}{P_{tot}} \tag{1}$$

where W is the total energy in the resonator and P_{tot} is the total power in the antenna. P_{tot} consists of the radiated power and the power loss in the antenna structure, as well as its surroundings. As mentioned earlier, as the size is reduced, the stored energy – especially in the near field –

Table 1 Frequency bands and antenna types used in commercial wireless systems [1]

Wireless technology	Frequency band	Antenna
GSM	880–960, 1710–1880 and 1850–1990 MHz	folded-F, patch, monopole
GPS	1227–1575	patch
Bluetooth, WLAN	2.4–2.5, 5.15–5.35 and 5.75–5.82 GHz	folded-F, patch, monopole

is increased and the radiated power is reduced, which results in a high quality factor resonator. As a result the bandwidth of the antenna is reduced and is given by

$$BW \equiv \frac{\Delta f}{f_{\text{res}}} \simeq \frac{1}{Q} \tag{2}$$

where Δf is the bandwidth and f_{res} is the resonant frequency of the resonator. It should be noticed that for electrically small antennas there is a trade-off between the size, bandwidth and efficiency. For simple electrically small linear and circular polarised antennas, a maximum bandwidth efficiency product can be derived based on the Chu–Harrington theory [3–6]. Here, the efficiency of the antenna is defined as $\eta = P_{\text{rad}}/P_{\text{tot}}$

$$\begin{aligned} (BW \cdot \eta)_{\text{MAX}} &\simeq [ka]^3 \text{ linear polarisation} \\ (BW \cdot \eta)_{\text{MAX}} &\simeq 2 \cdot [ka]^3 \text{ circular polarisation} \end{aligned} \tag{3}$$

It can be inferred that the maximum bandwidth efficiency product may be obtained when the antenna fills up completely the volume of the hypothetical sphere defined by Wheeler [2]. However, most integrated electrically small antennas have a planar structure based on a microstrip patch or PIFA antennas (Table 1) that are far from filling the bounding sphere. Their main advantages are that they are cheap and relatively easy to integrate. Moreover, for such antennas, there are many techniques available to reduce their size. However, for these types of antennas the maximum attainable bandwidth–efficiency is significantly lower than the theoretical limit. On top of that they usually have low efficiency because of metal losses and surface wave losses and also they can be very easily detuned, which in turn makes them more difficult to be integrated efficiently in personal communication systems. On the other hand, dielectric resonator antennas (DRAs) have no metal losses and the losses through surface waves in the substrate can be completely avoided if the dielectric constant is higher than that of the substrate itself. In addition, from the point of view of the Chu–Harrington limit on bandwidth–efficiency, DRAs offer the possibility of getting closer to the theoretical limit mainly because of their three-dimensional geometry, therefore the hypothetical Wheeler sphere can be utilised in a more optimised manner. The advantages of DRAs – such as high radiation efficiency, simple feeding schemes, resistance to detuning and relative small size – have been exploited at frequencies of several gigahertz or even higher [7]. For cellular applications in modern portable wireless systems, integration and implementation of DRAs is not straightforward. The main drawback is the relatively large size of the radiators when used at lower frequencies, such as 902–928 MHz or 2.400–2.500 GHz. Recently, some attempts to design and integrate a DRA of a reasonable size for these frequency bands have been reported [8], but the volume of the antenna is still quite large. In a recent work [9], the authors experimented with the implementation of a cylindrical DRA integrated at a package level into a fully functional Bluetooth module. Even though the newly developed module had much better performance – mainly because of the excellent attributes of the DRA implemented when compared with conventional technology such as a chip antenna – the overall volume of the radiator was not sufficiently small. To appreciate the volume occupied by a DRA with a dielectric constant of 20 with respect to the regular chip antenna usually used in such Bluetooth modules, a comparison of sizes is provided in Fig. 1.

New attempts to reduce the size of a DRA have recently been reported. Kishk [10] proposed the use of electric and magnetic conductors to reduce the size of the resonator. With such a technique, the size of the radiator can be reduced by up to 75%, but this will work only for certain resonating modes for which the perfect magnetic conductor condition (tangential component of H is zero) is fulfilled. Furthermore, this technique will result in a deformation of

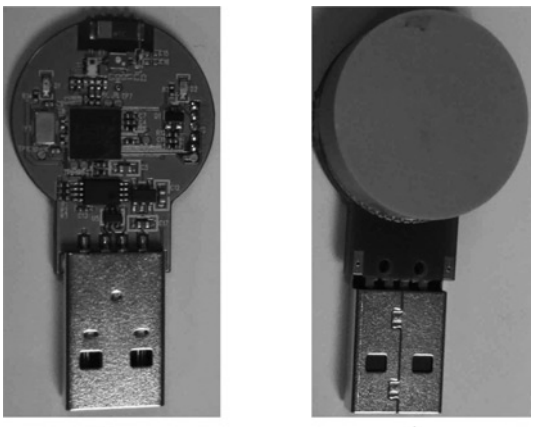

Figure 1 *Bluetooth module with electrically small antennas*

a Chip antenna (it can be seen at the top of the module)
b With integrated DRA (the cylindrical shaped ceramic resonator mounted on top of the module)

doi: 10.1049/iet-smt:20080122

the radiation pattern; however, this might be acceptable for applications such as personal communications in multipath environments. Another possibility to reduce the size of a resonator is to use a material with a vey high dielectric constant. This approach will reduce the size of the DRA but will result in an unacceptable reduction in bandwidth. As the dielectric constant increases, a rise of the quality factor (Q) of the resonator is observed. In fact Q increases as $\varepsilon^{3/2}$ thus resulting in significant reduction of the antenna bandwidth. Different methods have been suggested to improve the bandwidth of high dielectric constant resonator antennas [11].

A combination of two particular approaches appears promising. First, an appropriate resonator shape that minimises the surface to volume ratio is chosen. This is followed by a design of a resonator that can support close resonant modes. Another very important factor in wideband operation is the feeding structure design, such that efficient coupling is obtained for the desired resonant modes.

The design of a resonator supporting more than one resonant mode in close proximity is usually avoided in conventional DRA designs since the radiation pattern is strongly dependent on the resonator modes [12, 13]. However, the requirements for the polarisation and/or radiation pattern of antennas used in hand-held wireless systems are rather relaxed as they will usually be used in an indoor environment, which is in fact a multipath environment. For example, for an antenna to be used for the IEEE 802.11b,g band (2.4–2.5 GHz), the most important factor is that the bandwidth is well covered and the efficiency of the antenna is as high as possible (minimum 75%); then the next important factor is its size such that it can be integrated into the hand-held system. Another important fact that has to be taken into consideration from the system point of view is that the coupling between the antenna and the rest of the circuitry is avoided.

The points raised above were considered and implemented in the earlier work [9]. In this paper, a novel shape DRA is proposed to reduce the size of the radiator. The method used here is based on using a very high dielectric constant for the resonator combined with a novel shape resonator designed to support transverse electrical TE modes and quasi-TE modes excited by simple means of a 50 Ω open microstrip line. The open stub of the feed was used to tune the bandwidth of the antenna.

2 Antenna structure

As explained in the introduction, for practical hand-held applications at cellular frequencies, a compact DRA is preferred. One way of achieving a compact resonator is by using high permittivity materials. The Q factor of the antenna is the key parameter, which controls the bandwidth of the antenna (2). It can be directly related to the unloaded Q of the resonant mode excited in the dielectric resonator. The unloaded Q factor can be linked to the geometrical features of the resonator by the following equation

$$Q = 2\omega_0 \frac{\text{Stored energy}}{\text{Radiatedpower}} \propto 2\omega_0 \varepsilon_r^p \left(\frac{\text{Volume}}{\text{Surface}}\right)^s \quad (4)$$

with $p > s \geq 1$, where ω_0 is the resonant angular frequency and ε_r is the relative dielectric constant. From (4) it is apparent that an increase in ε_r will result in an increase of Q and this will reduce the antenna bandwidth. Moreover, it may be seen from (4) that – if the volume to surface ratio is minimised – the quality factor will be reduced and the bandwidth of the antenna increased.

Rectangular tile-shaped DRAs were studied and fabricated as reported in [11, 12]. It was demonstrated that thin rectangular DRAs have a wider bandwidth than cube-shaped or thick rectangular DRAs made from the same material at the same frequency. However, this study was limited to rectangular shape structures – more specifically to parallelepiped shapes, and even more specifically to a parallelepiped with 90° angles between all pairs of adjacent sides [12]. In this work, we wish to demonstrate that the idea is not limited to parallelepiped structures but can also be applied to cylindrical-based shapes. The results reported here are based on simulations only. We have simulated the structures published in [11, 12] and compared the performance with the simulation results obtained for the novel structure proposed here. These comparisons are included in Section 3 of this paper.

The novel shape proposed and studied here is a 'C' shaped resonator (Fig. 2) which has its thickness much smaller than all the other dimensions. The 'C' shaped resonator is a modification of a cylindrical resonator from which a circular segment has been removed. The rationale for this peculiar geometry will be explained in more detail in the following sections. Most of the previously published data regarding cylindrical resonators considered an arrangement with the resonator mounted on top of a grounded substrate with one

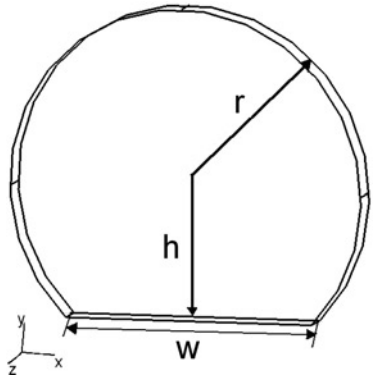

Figure 2 *'C' shaped resonator*

of the circular faces fixed to the substrate. In such a setup, only TM and quasi-TM modes are possible to be excited into the resonator. There is a lot of work done on cylindrical resonators [7–10, 14, 15], mostly on extracting approximate formulas to compute their resonant frequencies and quality factors. However, not much literature on cylindrical thin dielectric resonators (disk shape) and their properties exist. In a study done by Kishk and Glisson [15], the resonant frequencies and quality factors of cylindrical resonators for the first four dominant modes – namely $TM_{01\delta}$, $TE_{01\delta}$, $HEM_{11\delta}$ and $HEM_{12\delta}$ – as a function of different radius-to-height ratios and for different dielectric constant values, were measured and computed numerically. The ratios considered varied from 0.3 to 2.7 [15]. The aim was to obtain curve-fit equations for the data so that these equations could then be used to design any arbitrary sized cylindrical resonator. Two of the curve-fit equations for the resonant frequency of the $TE_{01\delta}$, $HEM_{12\delta}$ modes are quoted below

$$f_{\mathrm{TE}01\delta} = \frac{2.9 \cdot c}{2\pi \cdot r\varepsilon_{\mathrm{r}}^{0.46}}\left[0.7 + 0.3\frac{r}{t} - 0.03\left(\frac{r}{t}\right)^2\right] \quad (5)$$

$$f_{\mathrm{HEM}12\delta} = \frac{3.1 \cdot c}{2\pi \cdot r\varepsilon_{\mathrm{r}}^{0.5}}\left[1.2 - \left(0.04 - \frac{3.4}{\mathrm{e}^{2.6r/t}}\right)\frac{r}{t} + 1.55 \cdot \log\left(\frac{r}{t}\right)\right] \quad (6)$$

where r is the radius of the resonator and t its thickness.

Similar equations were derived for the other two modes $TM_{01\delta}$ and $HEM_{11\delta}$. An observation that came out from this study was that the rates of change in the resonant frequencies of the $TE_{01\delta}$ and $HEM_{12\delta}$ modes with respect to the radius-to-height ratio are lower than for the other two modes $TM_{01\delta}$ and $HEM_{11\delta}$. This implies that a DRA resonating with the $TE_{01\delta}$, $HEM_{12\delta}$ will possibly have a wider bandwidth than the same DRA working in the $TM_{01\delta}$, or $HEM_{11\delta}$ regime. Hence it may be desirable to create an appropriate DRA structure to support the $TE_{01\delta}$, $HEM_{12\delta}$ modes. For the knowledge of the near field distribution for each mode, it is necessary that an appropriate excitation mechanism is chosen.

Another method through which the resonant frequency of a cylindrical resonator can be approximately predicted is by using the cavity resonator model. In this approximation, the outer surfaces of the resonator are assumed to be perfect magnetic walls and the wave functions of the transverse electric TE and transverse magnetic TM, with respect to the z direction, can be written as

$$\psi_{\mathrm{TE}npm} = J_n\left(\frac{2X_{np}}{2 \cdot r}\rho\right)\left\{\begin{matrix}\sin n\varphi \\ \cos n\varphi\end{matrix}\right\}\sin\left[\frac{(2m+1)\pi z}{2t}\right] \quad (7)$$

$$\psi_{\mathrm{TM}npm} = J_n\left(\frac{2X'_{np}}{2 \cdot r}\rho\right)\left\{\begin{matrix}\sin n\varphi \\ \cos n\varphi\end{matrix}\right\}\cos\left[\frac{(2m+1)\pi z}{2t}\right] \quad (8)$$

where J_n is the Bessel function of the first kind, $J_n(X_{np}) = 0$, $J'_n(X'_{np}) = 0$, $n = 0, 1, 2, 3, \ldots$, $p = 1, 2, 3, \ldots$, $m = 0, 1, 2, \ldots$. From (7) and (8), and using the separation equation $k_\rho^2 + k_z^2 = \omega^2\mu\varepsilon$, one can find an expression for the resonant frequency of the npm mode

$$f_{npm} = \frac{c}{2\pi \cdot r\sqrt{\varepsilon_{\mathrm{r}}}}\sqrt{\left\{\begin{matrix}X_{np}^2 \\ X_{np}'^2\end{matrix}\right\} + \left[\frac{\pi \cdot r}{2t}(2m+1)\right]^2} \quad (9)$$

From (9) it can be deduced that for thin resonators – where the ratio of radius over thickness is much larger than unity – the second term $[(\pi \cdot r/2 \cdot t)(2m+1)]^2$ will dominate the first term $\left\{\begin{matrix}X_{np}^2 \\ X_{np}'^2\end{matrix}\right\}$ for small values of n and p which corresponds to first dominant modes. As a consequence the first resonant modes will be closely spaced together and it will be possible to design an antenna based on a multimode operation.

Both expressions quoted above (5) and (9) could be used to calculate the first resonant frequency of a cylindrical resonator. However, on close inspection, it can be noticed that when $2t/\lambda_g < 1$, where λ_g is the wavelength in the dielectric waveguide at the frequency of interest, these formulae produce erroneous results. As an illustration a simple example may be considered. Assume a cylindrical resonator with a high dielectric constant ε_{r} of 80. If the ratio of the radius of the resonator to its thickness is very high (more than 3), the results obtained using (5) are very different to the frequency computed by (9). However, when the ratio is reduced to 2, or below, the two methods give very similar results (Fig. 3). This is because for very thin resonators fields do not change rapidly enough in the z

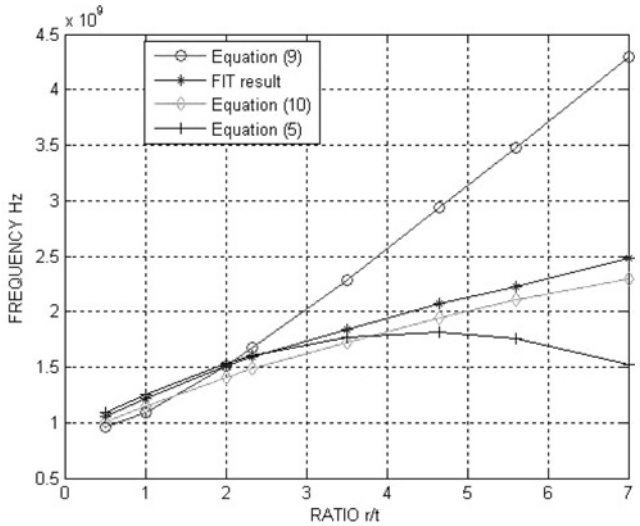

Figure 3 *TE_{01} resonant frequencies of cylindrical resonators with different radius over thickness ratio calculated using four different methods*

Dielectric constant of the resonator considered in this example was 80

doi: 10.1049/iet-smt:20080122

direction and no standing wave patterns appear along this direction. Therefore m should not necessarily be an integer number as defined earlier but it could be a real number between 0 and 1 to account for the thin feature of our resonator.

The basic operation of the $TE_{01\delta}$ mode can be explained if the dielectric resonator is considered as a short length (of thickness t) of a dielectric waveguide open at both ends. The lowest order TE mode of such a guide is the TE_{01} mode. Because of the high permittivity of the resonator, propagation along its thickness can occur inside the dielectric at the resonant frequency, but the fields will be cut off in the air regions around the dielectric. Since the resonant length for the $TE_{01\delta}$ mode is $< \lambda_g/2$, $\delta = 2t/\lambda_g < 1$ is used to denote the variation along the thickness of the resonator at this resonating mode. As the dielectric constant of the resonator is high, we can consider magnetic walls on all resonator faces. For these conditions, considering the TE mode implies $E_z = 0$ (along the thickness of the resonator). Furthermore, if we write the wave equation for H_z inside and outside the resonator with the magnetic walls boundary condition applied on all resonator faces, the following equation can be derived [16]

$$\tan\frac{\beta \cdot t}{2} = \frac{\alpha}{\beta} \tag{10}$$

where $\alpha = \sqrt{(X_{01}/r)^2 - k_0^2}$, $\beta = \sqrt{\varepsilon_r k_0^2 - (X_{01}/r)^2}$ and $k_0 = 2\pi f/c$. The above equation can be solved using the bisection method and thus the TE_{01} resonant frequency found.

To verify the solution numerically a simple experiment was conducted. Different cylindrical resonators with the dielectric constant fixed ($\varepsilon_r = 80$) and a radius of 14 mm were considered. The ratios of radius over thickness ranging from 0.5 to 7 were assumed and the resonant frequency for the TE_{01} mode was calculated using (5), (9) and (10). A numerical solution based on the finite integration technique (FIT) solver was also obtained for benchmarking. The results are presented in Fig. 3. As mentioned before, both (5) and (9) fail to predict the correct resonant frequency for ratios bigger than 3; (5) underestimates the correct solution whereas (9) grossly overestimates the resonant frequencies for thin resonators. On the other hand, the solution based on the transcendental equation (10) computes frequencies that are slightly underestimated when compared with the full wave solution obtained from the FIT solver but nevertheless consistent over the whole range of ratios. Therefore for a correct approximation of the resonant frequency of the lowest resonant mode $TE_{01\delta}$ for a disk shaped resonator, it is necessary to solve the transcendental equation (10), or an even better alternative is to use a full wave solver.

Equation (10) can be used to calculate the size of the resonator if the band of the antenna is known. For example, if the DRA is to be used for a Bluetooth application, the first resonant mode of the resonator should be around 2.4–2.5 GHz. If, for example, the ceramic used has a dielectric constant of 80 and the thickness available (which, from the system point of view, is 2 mm), then the radius of the resonator will be 14 mm. If, however, the radius has to be constrained from the system point of view, say reduced to 10 mm, then when using the same material the thickness of the resonator should be increased to 3 mm to get a resonant frequency close to 2.4 GHz.

The near field distribution of the lowest resonant modes can be obtained from the full wave solver. It is clear from the electric field plots (Fig. 4) that the feed and the ground have to be positioned with respect to resonator in such a way that the magnetic field produced by the feed will be orthogonal to the circular faces of the resonator. This is not as easily achievable for a cylindrical shape as for a parallelepiped shape [11, 12]; however, a simple solution such as the one proposed here could be employed. If the

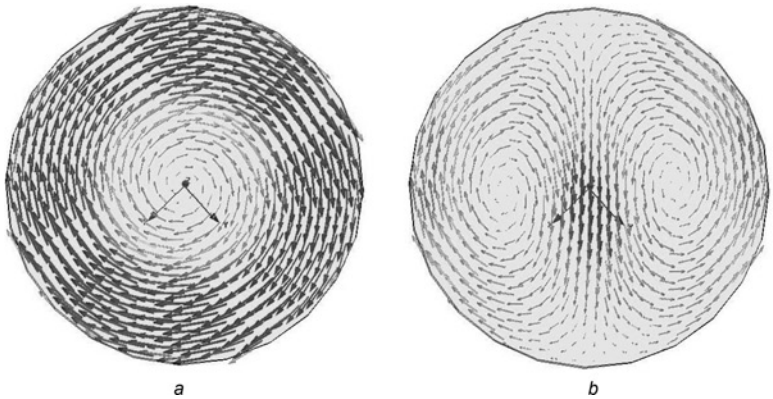

Figure 4 *Electric field distribution for the first two resonant modes of a thin cylindrical dielectric resonator*

a $TE_{01\delta}$
b $TE_{11\delta}$

cylindrical resonator were transformed into a 'C' shaped resonator, the feed problem would become very simple and easy to implement; it would in fact yield similar results as for the parallelepiped shape patented by Bit-Babik *et al.* [12].

The first resonant mode of the 'C' shaped resonator is $TE_{01\delta}$. The resonant frequency of this mode can be approximated using the same method as described earlier. The difference appears in the definition of α and β which have to take into account the change in the resonator volume. If a variable ν = Volume rmdisk/Volume 'C' shaped is defined, then α and β can be written as

$$\alpha = \sqrt{(\nu \cdot X_{01}/r)^2 - k_0^2},\ \beta = \sqrt{\varepsilon_r k_0^2 - (\nu \cdot X_{01}/r)^2} \quad (11)$$

For a radius $r = 14$ mm, thickness $t = 2$ mm and $h = 10$ mm, where h is the distance from the centre of the circular face to the middle of the flat edge as shown in Fig. 2, the variable defined above becomes $\boldsymbol{\nu} = 1.096$. With this value the approximate resonance of the $TE_{01\delta}$ of the 'C' shaped resonator ($\varepsilon_r = 80$) is calculated to be at 2.42 GHz. Again, as in the cylinder calculation, the approximate value compares well with the value of 2.53 GHz computed through the FIT solver, being only slightly lower. Fig. 5 presents a comparison between the resonant frequencies computed using (10) and computed through the FIT solver for different ratios $\boldsymbol{\nu}$.

The near field distribution within the 'C' shaped resonator is very similar to the full cylinder. The vector electric field plots for the first three resonant modes obtained from the full solver software are shown bellow.

To couple the modes presented in Fig. 6, a simple microstrip line feed would suffice. As shown in Bit-Babik's work [11, 12] the resonator has to be placed on top of the microstrip line, parallel with the line (Fig. 7). In this configuration, the magnetic field lines produced by the current flowing into the microstrip line will close through the 'C' shaped faces of the resonator. By placing the flat face of the resonator on top of the metallic microstrip line, the boundary condition of that face is changed from perfect magnetic to perfect electric. This will influence the field distribution of the field inside the resonator. The resonant frequencies of first modes are also changed. A simple analytical approach is not possible in this case, as the problem loses its inherent circular symmetry, therefore a numerical tool is employed to compute the first resonant modes of this arrangement (Fig. 7*b*). Under these circumstances, the problem has a perfect magnetic boundary around the circumference of the resonator and a perfect electric boundary along the straight bottom boundary.

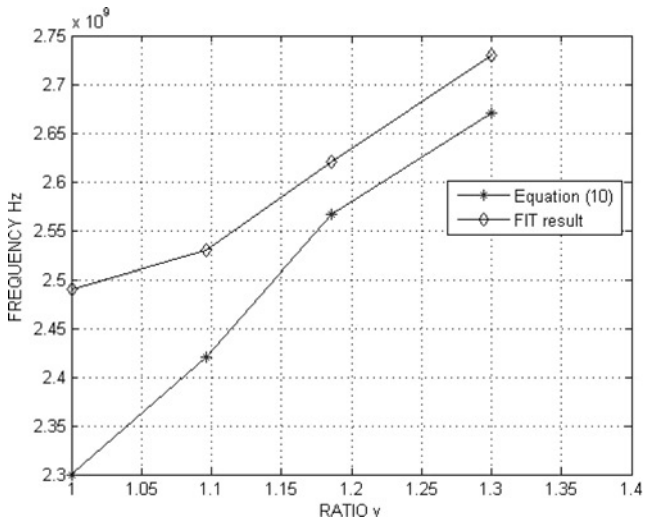

Figure 5 *Resonant frequencies for the $TE_{01\delta}$ of the 'C' shaped resonator for different $\boldsymbol{\nu}$ – volume ratios*

The new electric field plots are presented in Fig. 8. The computed resonances of the first three modes are 1.87 GHz for the TE_{01} mode (Fig. 8*a*), 2.79 GHz for the TE_{12} mode (Fig. 8*b*) and 2.88 GHz for the TE_{11} mode (Fig. 8*c*).

It can also be shown that the first resonant frequency of the 'C' shaped resonator with the flat face shortened (Fig. 7*b*) is related to the first resonant of the complete cylinder resonator, which has the same circular sector that is removed for the 'C' shaped resonator shortened through the same coefficient ν = Volume disk/Volume 'C' shaped (Fig. 7*a*). The actual antenna structure is presented in Fig. 9. The flat portion of the resonator is fixed above the microstrip line that is routed on top of the grounded substrate supporting the whole antenna structure. The microstrip line becomes a simple and efficient feed for the 'C' shaped DRA.

The microstrip feeds are in general not the most efficient way to couple the energy into a ceramic resonator, but because the dielectric constant of this particular implementation is very high such problems are avoided. The dielectric material considered here has the dielectric constant of $\varepsilon_r = 80$ and the loss tangent of 0.0005 at 2 GHz, but higher values of dielectric constants such as 100 or 120 could also be appropriate. This kind of a resonator could be fabricated using ceramic materials based on $BaTiO_3$ compounds that provide a wide range of high permittivity and low loss. Depending on the sintering conditions and various binders added, the values of the dielectric constants between 50 and 200 could be achieved. Other materials are also available such as neodymium titanate and magnesium calcium titanate [14].

3 Results and discussions

As mentioned earlier, all results generated throughout this work are from numerical simulations. However, for the purpose of increasing confidence in the results, two commercially available software packages, using two

doi: 10.1049/iet-smt:20080122

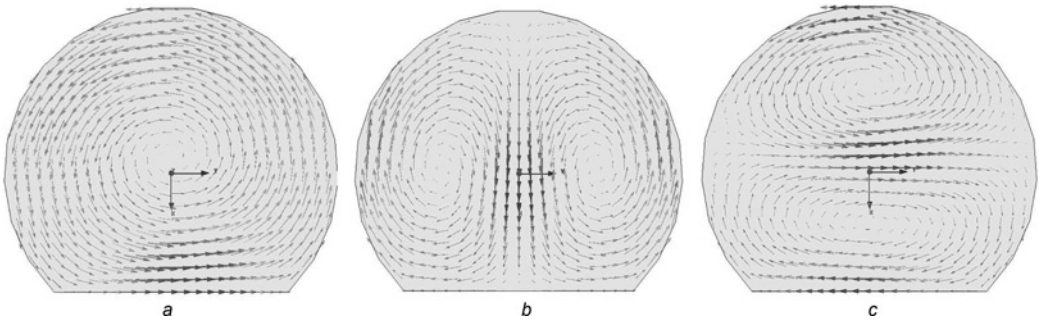

Figure 6 *Electric field distribution in the 'C' shaped resonator for the first three resonant modes*

a $TE_{01\delta}$
b $TE_{11\delta}$
c $TE_{12\delta}$

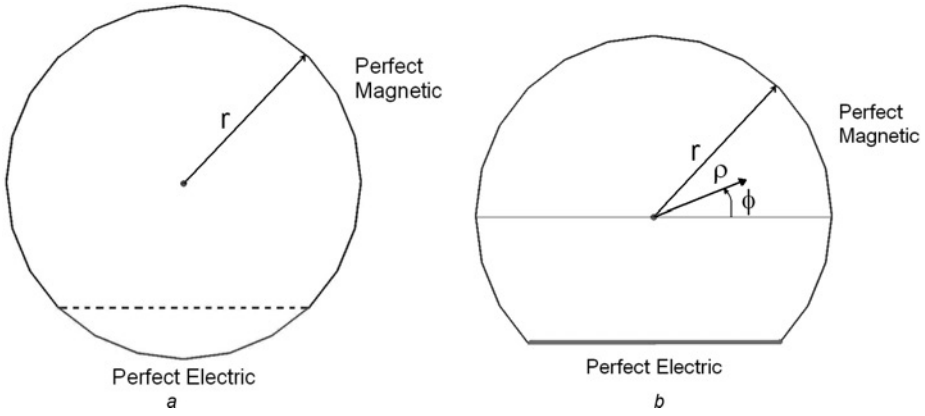

Figure 7 *The boundary setup for the case of the 'C' shaped resonator sitting on top of the microstrip line*

different methods, were used to simulate the same structure. The two packages were Microwave Studio from CST [17] and HFSS from Ansoft [18]. Microwave Studio employs a time-domain technique known as FIT, whereas HFSS uses a frequency-domain technique based on the finite element method (FEM). Both of are full wave solvers and generate results in terms of scattering (*S*) parameters from the field solution. Access to the field plots (electric and magnetic) is also possible. The results for the same structure were compared in terms of *S* parameters. The main difference between the two packages – as already mentioned – is that Microwave Studio solves the problem time domain whereas HFSS does it in frequency domain. The CST software was set up to first adapt its rectangular mesh until the error between successive solutions became $<1\%$. Once the adaptive mesh was obtained a simulation with an accuracy of better than -30 dB was initiated. As the code solves the problem in time domain, this accuracy refers, in practice, to the steady state reached after the initial Gaussian pulse has passed through the structure being simulated. This value is in fact the accuracy of the frequency-domain signals that are calculated by Fourier transformation of the time signals.

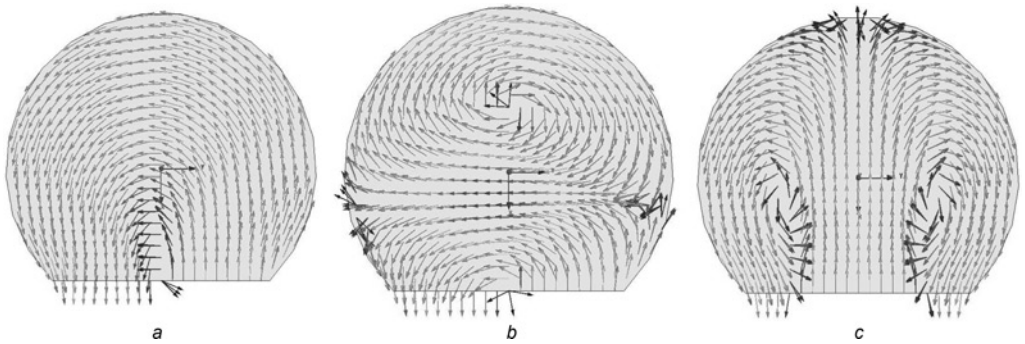

Figure 8 *Electric field distribution of the first three resonant modes in the 'C' shaped resonator in the new configuration*

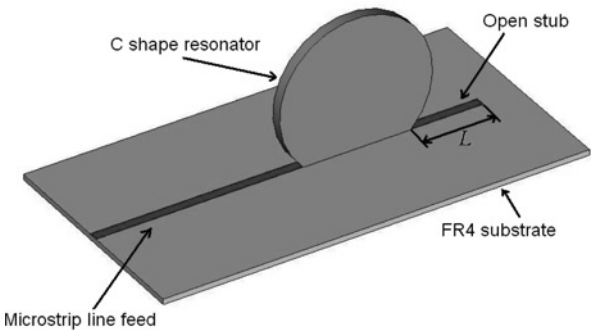

Figure 9 *'C' shaped resonator on top of a microstrip feed*

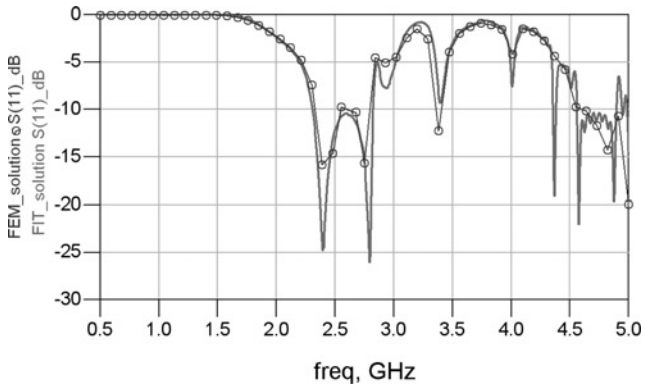

Figure 10 *Comparison between FIT and FEM solutions showing the magnitude of S11*

The Ansoft software, on the other hand, was set up to iterate the mesh until an error of $<1\%$ at the input has been achieved. As this tool solves the problem in frequency domain, a frequency of 5 GHz was chosen to adapt the mesh until the error obtained at the input port became $<1\%$. The problem was then solved at 50 discrete points in the domain 0.5 to 5 GHz using the mesh adapted at 5 GHz. Fig. 10 shows a comparison in terms of the magnitude of return loss for one of the simulated cases, which has been solved with both solvers.

The antenna structure depicted in Fig. 9 was further investigated with the help of both solvers. Using the methodology described in Section 2, the initial dimensions of the resonator were chosen as follows: $r = 14$ mm, $h = 10$ mm and the thickness $t = 2$ mm (using $\varepsilon_r = 80$ and loss tangent of 0.0005 at 2 GHz, as specified before). As mentioned earlier, the first resonance of the 'C' shaped resonator placed on top of the microstrip is expected to be around 1.9 GHz (calculated in Section 2). The full wave results have confirmed this and when the length of the open stub at the end of the resonator was taken as $L = 0$, the first resonance observed was indeed at 1.97 GHz, as shown in Fig. 11*a*. The second resonance is around 2.78 GHz and the third one is 2.88 GHz, as predicted in Section 2. Because the second and third resonances are very close to each other, they form a continuous band from 2.7 to 2.9 GHz. A closer inspection of the electric field plots reveals that the first three resonances are the same as the ones described before (Figs. 11*b*–11*d*).

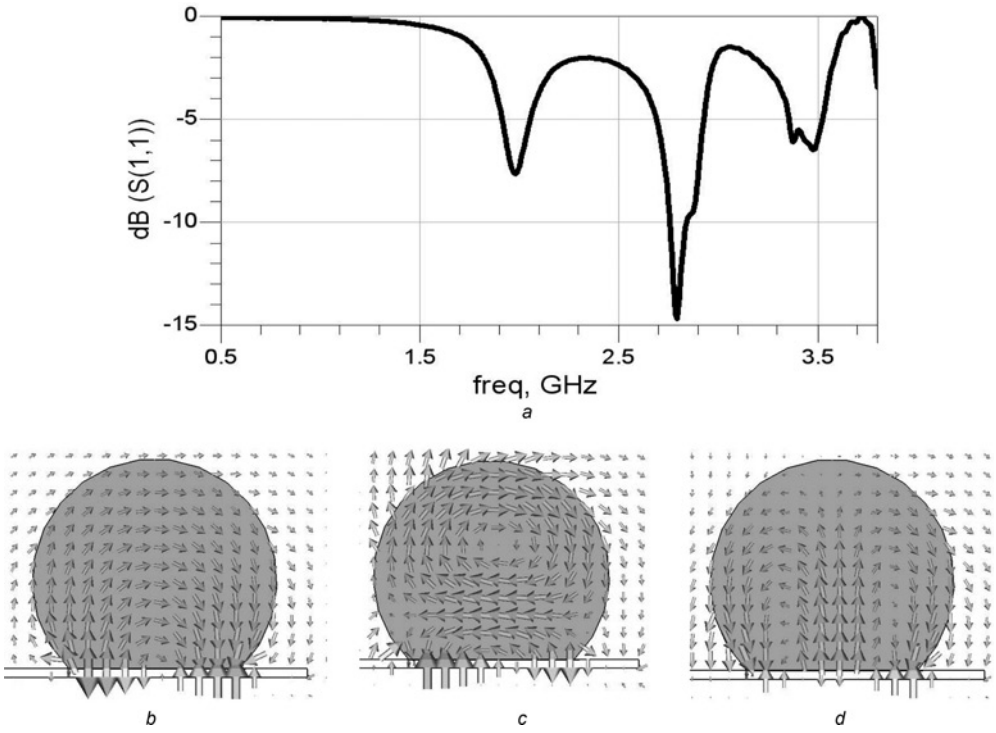

Figure 11 *Magnitude of S11 and the near field distribution of the first three resonant modes for the DRA antenna when L = 0*

doi: 10.1049/iet-smt:20080122

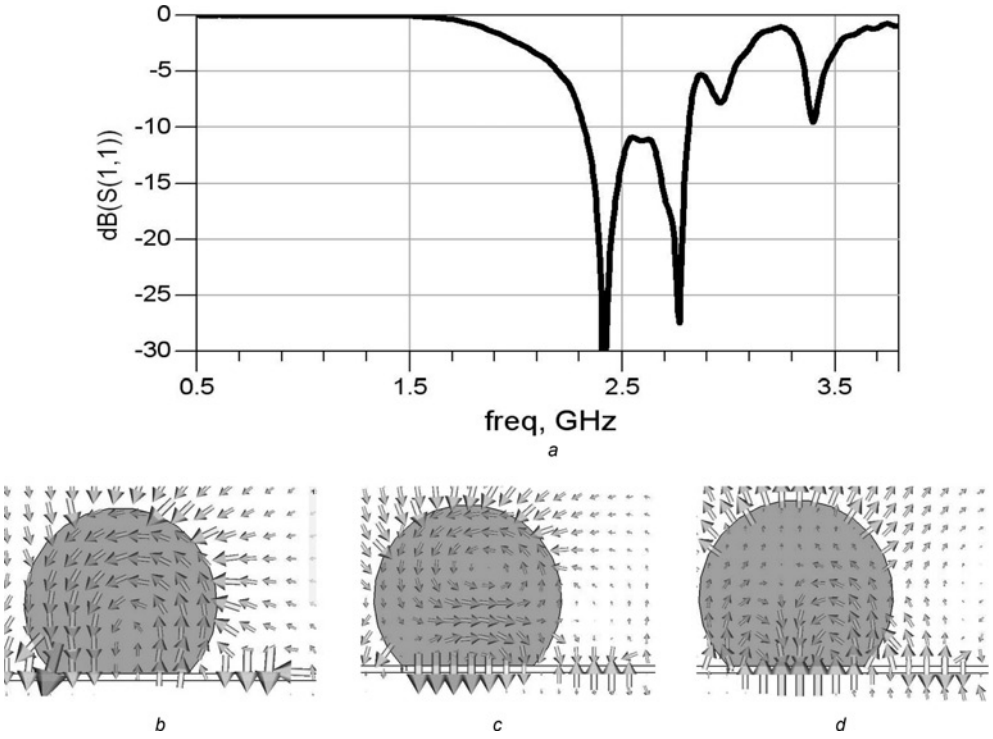

Figure 12 *Magnitude of S11 and the near field distribution of the first three resonant modes for the DRA antenna when $L = 13$ mm*

To increase the bandwidth of the antenna, one of the first two resonant modes has to be shifted towards the other one to create a continuous band in which the magnitude of $S11$ is below -10 dB. However, for this structure an interesting phenomenon has been observed, namely that the first resonant mode is due to the combined effects of the resonator and the length of the transmission line routed on the flat side of the resonator used to excite the antenna. When the length of the microstrip line is equal to the length of the flat side of the 'C' shaped resonator W ($L = 0$), the resonant frequency is around 1.9 GHz as predicted in Section 2 and shown in Fig. 11*a*. However, when the length of the transmission line exceeds W ($L > 0$), the resonant frequency is shifted upwards. Thus, a simple and efficient way to increase the bandwidth is through controlling the field distribution along the open stub. This can be achieved by varying the length of the stub accordingly. It is known that current density along the microstrip open stub will have a peak at $\lambda_g/4$, where λ_g is the wavelength of the guided wave along the microstrip line. By choosing the appropriate length, the intensity of the magnetic and electric field can be controlled so that the energy coupled with the resonator is maximised. In this case we know that the resonator has its natural resonance around 2.45 GHz. Using this information, an open stub can be designed such that a maximum of the magnetic (or electric) field will exist at one end of the resonator and another maximum – but with the opposite phase – will exist at the other end of the resonator. The $\lambda_g/4$ is around 16 mm for the microstrip line on FR4 at 2.45 GHz. The length of the flat surface $w = 20$ mm, hence by adding an open stub of $L = 13$ mm, the maximum field will appear at about 3 mm inside the right-hand side of resonator. The other maximum field region exists on the left-hand side of the resonator, where the excitation is as shown in Fig. 12*b*. In this arrangement the coupling of energy from the feed into the resonator, when the TE_{01} mode naturally exists, is maximised and a deep resonance at 2.41 is observed (Fig. 12). Moreover, the addition of L at the end of the feed does not disturb the field distribution at 2.77 GHz (Fig. 12*c*), which is the resonance of the second mode. This explains why by changing the length of the stub only the first mode is changing position, while the second mode stays fixed at around 2.79 GHz. The third mode is also influenced by the length of the open stub, as may be observed in Fig. 12. It appears at around 2.96 GHz but the energy is not coupled efficiently into the resonator and the resonance observed is not very pronounced.

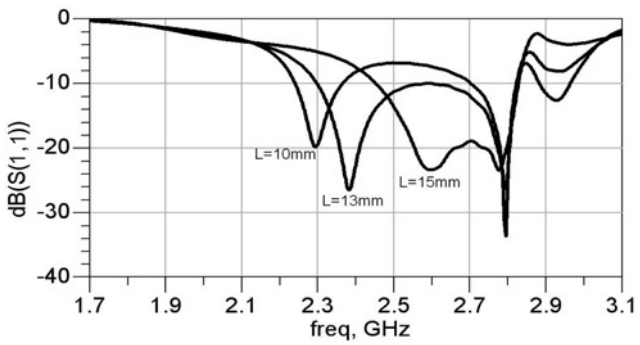

Figure 13 *Magnitude of S11 for different values of L*

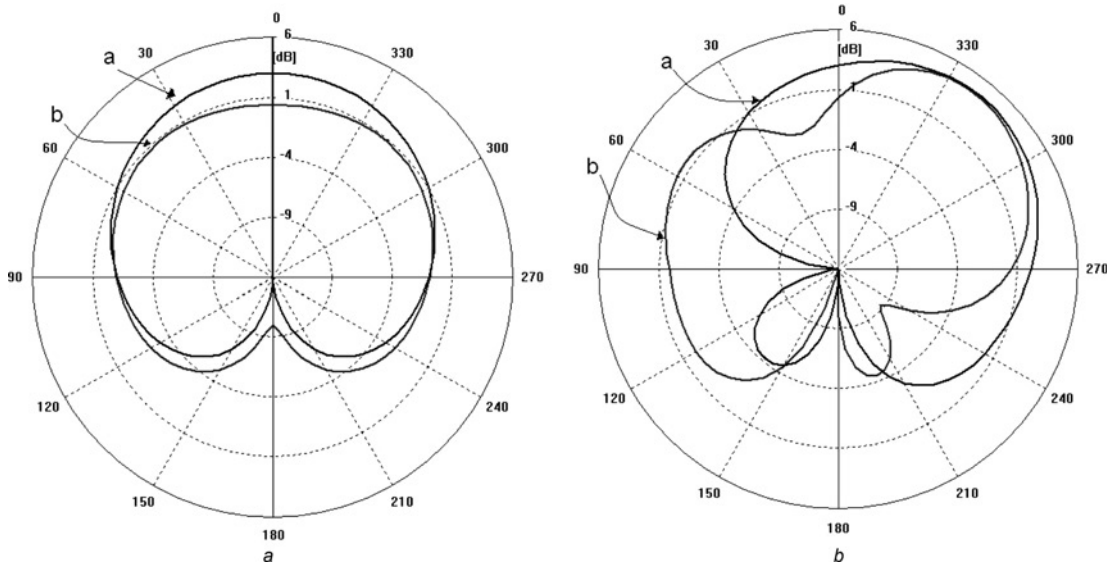

Figure 14 *Simulated radiation patterns for the two different modes in H and E plane*

a Pattern at 2.41 GHz (first mode)
b Pattern at 2.77 GHz (second mode)

The effect of changing the length of the open stub is further illustrated in Fig. 13. The length of the stub was varied from 10 to 20 mm to find an optimum length so that the bandwidth of the antenna is maximised. The length of about 13 mm seems to be optimal, whereas the 500 MHz – from 2.3 GHz to about 2.8 GHz – appears to be the maximum bandwidth achievable for this structure (Fig. 13).

The antenna presented here can be considered an electrically small antenna as its biggest dimension (diameter) is smaller than one-fourth of the free space wavelength corresponding to the lowest frequency mode of operation. In the case computed above the diameter is 28 mm and the free space wavelength at 2.4 GHz is 125 mm. For this type of structure the size of the ground plane is also very important. The ground plane reduces the power radiated in one hemisphere and produces some directionality in the radiation pattern in the other hemisphere. From the simulations, it has been observed that the ground plane should have the width at least equal to the diameter of the resonator in order to reduce substantially the radiation in one hemisphere. More improvements in the directivity of the antenna could be accomplished if the ground plane was increased further, but little improvement has been observed when the width of the ground was bigger than three times the radius of the antenna. The simulated radiation patterns in Fig. 14 have been obtained from a model that has a finite ground plane with a width twice the diameter and the length three times the diameter of the resonator (56×84 mm^2).

The gain and radiation efficiency of the antenna was also calculated. A very high efficiency was obtained for this structure for both modes, with the computed values above 95%. It should be noted that the metal losses in the microstrip line were ignored in the calculations, but these are expected to be very small and should not affect the efficiency of the DRA. The computed gain was for both modes better than 4.4 dB.

The proposed antenna was compared in terms of its bandwidth and radiation pattern with the parallelepiped DRA described by Bit-Babik *et al.* [11, 12]. The model that has been simulated here is identical with the DRA described in [11] and has the length of 25 mm, the height of 23 mm and the thickness of 2 mm with the dielectric constant of 80. The size of the ground plane considered here was 60×80 mm^2. For these dimensions, the volume of the parallelepiped was 1150 mm^3, whereas the volume of the 'C' shaped resonator is slightly smaller at 1123 m^3. The calculated bandwidth of parallelepiped DRA is also slightly smaller than for the proposed DRA as shown in Fig. 15. The main difference between the two antennas is in their

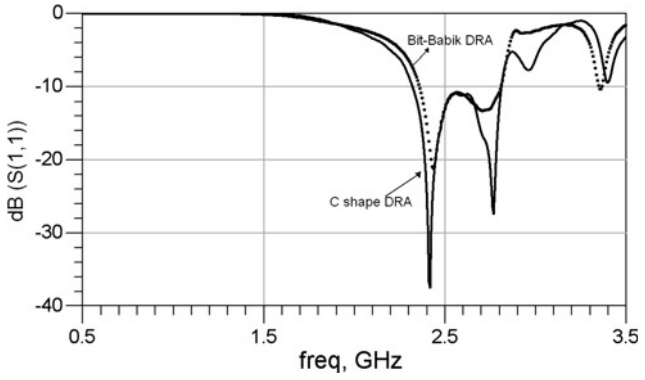

Figure 15 *Magnitude of S11 for parallelepiped and 'C' shaped DRAs*

doi: 10.1049/iet-smt:20080122

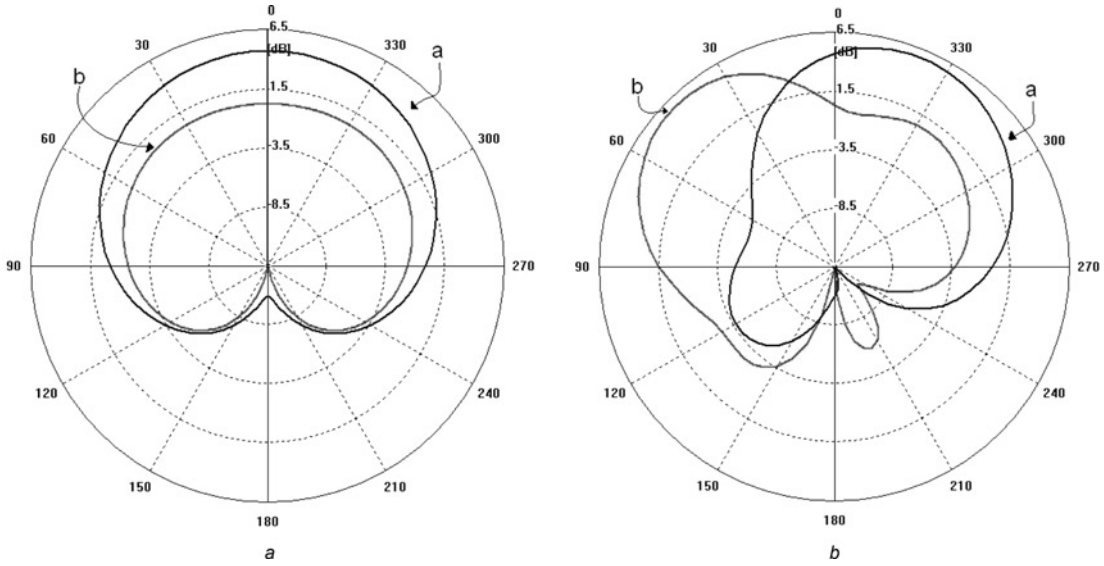

Figure 16 *Simulated radiation patterns for the two different modes in H and E plane – parallelepiped DRA*

a Pattern at 2.41 GHz (first mode)
b Pattern at 2.77 GHz (second mode)

radiation patterns, especially in the *E* plane. For the C shaped implementation both resonant modes have the maximum field positioned towards the same direction (Fig. 14), whereas the parallelepiped DRA has the maximum for the first resonant mode in opposite direction when compared with the second resonant mode (Fig. 16). This can be explained by the nature of the second mode excited in the resonators. The second mode for the parallelepiped resonator is the TE_{12} mode (two nulls along the length of the resonator), whereas the mode excited in the 'C' shaped resonator has two nulls along its height (Fig. 12*c*). This might be an advantage for the 'C' shaped resonator as the directivity of the mode does not change as dramatically as for the parallelepiped shape; however, in the implementation of a small antenna for hand-held wireless for indoor applications, this fact is of secondary importance.

4 Conclusions

A 'C' shaped high permittivity DRA has been studied through numerical modelling. It has been shown that by using a high enough permittivity material, and by selecting an appropriate shape of the resonator coupled with a multimode operation, a compact and wide bandwidth antenna for cellular frequencies could be realised. Further improvements of the size and bandwidth may be possible if higher dielectric constant is used and other shapes that minimise better the volume to surface ratio are employed. Finally, the DRAs have a fundamental advantage over the classical electrically small antennas as they are resonating without the need of an external reactive component (matching network). This will result in a more efficient antenna and will also facilitate the integration into a real wireless system.

5 References

[1] POZAR D.M.: 'An overview of wireless systems and antennas'. Proc. IEEE Antennas and Propagation Int. Symp. APS 2000, July 2000, vol. 2, pp. 16–21

[2] WHEELER H.A.: 'Fundamental limitations of small antennas', *Proc. IRE*, 1947, **35**, pp. 1479–1484

[3] CHU L.J.: 'Physical limitations on omni-directional antennas', *J. Appl. Phys.*, 1948, **19**, pp. 1163–1175

[4] HARRINGTON R.F.: 'Effect of antenna size on gain, bandwidth, and efficiency', *J. Res. Natl. Bur. Stand*, 1960, **64D**, pp. 1–12

[5] MCLEAN J.S.: 'The radiative properties of electrically-small antennas'. IEEE Int. Symposium on Electromagnetic Compatibility, 1994, pp. 320–324

[6] MCLEAN J.S.: 'A re-examination of the fundamental limits on the radiation Q of electrically small antennas', *IEEE Trans. Antenna Propag.*, 1996, **44**, (5), pp. 672–676

[7] LONG S.A., MCALLISTER M., SHEN L: 'The resonant cylindrical dielectric cavity antenna', *IEEE Trans. Antenna Propag.*, 1983, **31**, (3), pp. 406–412

[8] GAO Y., OOI B.-L., EWE W.-B., POPOV A.P.: 'A compact wide band hybrid dielectric resonator antenna', *IEEE Microw. Wirel. Compon. Lett.*, 2006, **16**, (4), pp. 227–229

[9] ROTARU M.D., LIM Y., KURUVEETTIL H., YANG R., POPOV A.P., CHUA C.-P.: 'Implementation of package integrated antenna with

embedded front end for Bluetooth applications', *IEEE Trans. Adv. Packag.*, 2008

[10] WEI HUANG K.A.A.: 'Use of electric and magnetic conductors to reduce the DRA size'. Int. Workshop on Antenna Technology: Small and Smart Antennas Metamaterials and Applications, IWAT '07, 2007

[11] BIT-BABIK G., DI NALLO C., FARONE A.: 'Multimode dielectric resonator antenna of very high permittivity'. IEEE Antennas Propagation Society Int. Symp, 2004, vol. 2, pp. 1383–1386

[12] BIT-BABIK G., DI NALLO C., FARONE A., BALZANO Q., ZARIDZE R.: 'Broad band and multi band antenna'. USPTO – 6,801,164 B2, October 2004

[13] MONGIA R.K., ITTIPIBOON A.: 'Theoretical and experimental investigation of rectangular dielectric resonator antennas', *IEEE Trans. Antenna Propag.*, 1997, **45**, (9), pp. 1348–1356

[14] MONGIA R.K., BHARTIA P.H.: 'Dielectric resonator antennas – a review and general design relations for resonant frequency and bandwidth', *Int. J. Microw. Millim.-Wave Comput. Aided Eng.*, 1994, **4**, (3), pp. 230–247

[15] KISHK A.A., GLISSON A.W.: 'Bandwidth enhancement for split cylindrical dielectric resonator antennas'. Progress in Electromagnetic Research, PIER 33, 2001, pp. 97–118

[16] POZAR D.M.: 'Microwave engineering' (John Wiley and Sons Inc., 2005, 3rd edn.), pp. 287–290

[17] www.cst.com

[18] www.ansoft.com

doi: 10.1049/iet-smt:20080122